Binding and Orientation of Conantokins in PL Vesicles and Aligned PL Multilayers†

Qiuyun Dai, Jaroslav Zajicek, Francis J. Castellino, and Mary Prorok*

Department of Chemistry and Biochemistry and the W. M. Keck Center for Transgene Research, University of Notre Dame, Notre Dame, Indiana 46556

Received May 29, 2003; Revised Manuscript Received August 25, 2003

ABSTRACT: The association of a ligand with its cognate cell surface receptor can be facilitated by interactions between the ligand and the lipid phase of the cell membrane. With respect to the *N*-methyl-D-aspartate receptor (NMDAR), we have previously established a low affinity, nonreceptor-mediated interaction of the peptidic conantokins with synaptic membranes in conjunction with a high affinity binding to the NMDARs present therein [Klein, R. C., Prorok, M., and Castellino, F. J. (2003) *J. Pept. Res. 61*, 307−317]. In the current study, several techniques including size-exclusion chromatography, circular dichroism, fluorescence, and NMR spectroscopies were used to investigate the binding, conformation, and orientation of conantokins and their variants to a variety of phospholipid (PL) vesicles and multilayers. We have found that conantokins bind to PLs and that the effectors Ca^{2+} and spermine slightly increase this binding ability. The conantokins preserve a high degree of helical conformation when bound to vesicles in the presence of Ca^{2+}. In the absence of Ca^{2+}, only conantokin-G (con-G) manifests an increase in conantokin helicity with increasing vesicle concentration. In solution, the conantokins appear to be localized at the headgroup of vesicles and do not insert into the hydrophobic core of the bilayer. On aligned PL films, the helical axis of the conantokins can either reside normal to the membrane surface or partition in a parallel orientation, depending on the nature of the conantokins and the PLs used. These orientation preferences may be conjoined with the biological activities of the conantokins.

Conantokins are short (17−27 amino acid residues), helical, γ-carboxyglutamate (Gla)[1]-rich peptides derived from the venoms of predatory marine cone snails. Four members of this family have been identified to date: conantokin (con)-G, con-T, con-R, and con-L (*1*−*4*). Physiologically, they act as potent and selective inhibitors of the *N*-methyl-D-aspartate receptor (NMDAR), a ligand-gated ion channel implicated in the integration and processing of information related to learning and memory. NMDAR dysfunction has been linked to many neuropathological disorders, including Alzheimer's disease, epilepsy, and ischemic cell death. With respect to the treatment of NMDAR-related pathophysiologies, recent animal model studies have demonstrated that the conantokins and their derivatives offer the promise of therapeutic efficacy without the neurobehavioral side effects that attend the use of many NMDAR antagonists (*3*−*6*).

In a previous study, we examined the binding of radiolabeled conantokins to the NMDARs present in crude rat brain membrane suspensions and found a significant, albeit weak (ca. 7 μM), nonreceptor component to the displaceable binding (*7*). Such adhesion of conantokins to brain membranes may be analogous to Ca^{2+}-mediated binding of Gla-containing coagulation proteins to the membrane surface. This translocation event is required at numerous steps in the clotting cascade and is routinely modeled with acidic phospholipid (PL)[1] vesicles (*8*−*11*). In a similar vein, it has recently been reported that the interaction of the Gla-containing gas6 ligand for its cognate receptor on photoreceptor outer segments is incumbent upon and preceded by Ca^{2+}-triggered binding of the gas6 Gla domain to membrane PLs (*12*). We suggest that this apparently general mechanism of Gla-dependent adhesion to the plasma membrane is operant in the action of the native conantokins, owing to their high relative content of Gla, and may function to facilitate their involvement with the NMDAR target. The accumulation of peptide ligands at the membrane surface has been observed for several peptide−receptor classes and has been postulated to increase the effective concentration of the peptide ligand in the vicinity of the receptor and induce preferred ligand conformations (reviewed in ref *13*). Collectively, these considerations prompted us to examine the interaction of

† Supported by National Institutes of Health Grant HL-19982 (to F.J.C.) and an American Heart Association Scientist Development Grant (to M.P.).

* To whom correspondence should be addressed. Tel: (574) 631-9120. Fax: (574) 631-8017. E-mail: mprorok@nd.edu.

[1] Abbreviations: AFM, atomic force microscopy; BLPC, bovine liver phosphatidylcholine; Gla, γ-carboxyglutamic acid; PL, phospholipid; PC, L-α-phosphatidylcholine (L-α-lecithin); CD, circular dichroism; DOPC, 1,2-dioleoyl-*sn*-glycero-3-phosphocholine; DOPS, 1,2-dioleoyl-*sn*-glycero-3-[phospho-L-serine]; DOPG, 1,2-dioleoyl-*sn*-glycero-3-[phospho-DL-(1-glycerol)]; DMPC, 1,2-dimyristoyl-*sn*-glycero-3-phosphocholine; DMPC-d_{54}, 1,2-dimyristoyl-d_{54}-*sn*-glycero-3-phosphocholine; DMPS, 1,2-dimyristoyl-*sn*-glycero-phospho-L-serine; DMPS-d_{54}, 1,2-dimyristoyl-d_{54}-*sn*-glycero-phospho-L-serine; DSS, 3-(trimethylsilyl)-1-propane-sulfonic acid; NOESY, nuclear Overhauser effect spectroscopy; T_1, spin−lattice (longitudinal) relation time; T_2, spin−spin (transverse) relaxation time; TFA, trifluoroacetic acid; TOCSY, total correlation spectroscopy; DQF−COSY, double quantum filtered correlation spectroscopy.

10.1021/bi034918p CCC: $25.00
Published on Web 10/11/2003

conantokins with model PL membranes, with emphasis on orientation on the PL, as it may relate to NMDAR inhibition. The present study reports the binding properties, structural tendencies, and orientation of several conantokins in the presence of PL vesicles and oriented multilayer films of varying peptide/PL composition.

MATERIALS AND METHODS

Materials. BLPC, DOPC, DOPS, and DOPG were purchased from Sigma (St. Louis, MO), while DMPC-d_{54} and DMPS-d_{54} were obtained from Avanti Polar Lipids, Inc. (Alabaster, AL).

Peptide Synthesis, Purification, and Characterization. Peptides were synthesized on a 0.1 mmol scale as described previously (*14*) on PAL resin support (Applied Biosystems, Fullerton, CA) using an Applied Biosystems model 433A peptide synthesizer. The synthesis of N^{α}-Fmoc-(γ,γ'-di-*O*-*t*Bu)-L-Gla, the ^{13}C isotopically enriched [δ,δ-di-^{13}C]-N^{α}-Fmoc-(γ,γ'-di-*O*-*t*Bu)-L-Gla, and [γ-^{13}C]-N^{α}-Fmoc-(γ,γ'-di-*O*-*t*Bu)-L-Gla was accomplished as reported earlier (*15*). The FPLC purifications of conantokin peptides were performed using a Bioscale DEAE20 anion exchange column (Bio-Rad Laboratories, Hercules, CA) equilibrated with 10 mM sodium borate, pH 7.80. After loading, the peptides were eluted with a 500 mL linear gradient beginning at 10 mM sodium borate to a limit of 10 mM sodium borate/500 mM NaCl, pH 7.80. The target peptide was pooled, lyophilized, and desalted on a column of Sephadex G-15 (Sigma Chemical Co., St. Louis, MO) equilibrated in 0.1% NH_4OH. The peptides were characterized by reverse-phase HPLC and DE-MALDI-TOF mass spectrometry on a Voyager-DE spectrometer (PerSeptive Biosystems, Framingham, MA) as reported previously (*14*). The amino acid sequences of the peptides used in this study are as follows (residues in boldface denote variations from the primary sequence of the parent peptide):

con-G: G E γ γ L^5 Q γ N Q γ^{10} L I R γ K^{15} S N-NH$_2$

con-G[S16Y]: G E γ γ L^5 Q γ N Q γ^{10} L I R γ K^{15} **Y** N-NH$_2$

con-G/Ala: G E γ γ L^5 **G K A** Q **A**^{10} L I R **A A**^{15} **A A**-NH$_2$

con-G/Ala[A16Y]: G E γ γ L^5 **G K A** Q **A**^{10} L I R **A A**^{15} **Y A**-NH$_2$

con-T: G E γ γ Y^5 Q K M L γ^{10} N L R γ A^{15} E V K K N^{20} A-NH$_2$

con-T[Y5W]: G E γ γ **W**^{5} Q K M L γ^{10} N L R γ A^{15} E V K K N^{20} A-NH$_2$

con-T[K7W]: G E γ γ Y^5 Q **W** M L γ^{10} N L R γ A^{15} E V K K N^{20} A-NH$_2$

con-R17: G E γ γ V^5 A K M A A^{10} γ L A R γ^{15} N I-NH$_2$

con-R17[V5Y]: G E γ γ **Y**^{5} A K M A A^{10} γ L A R γ^{15} N I-NH$_2$

con-R17/Ala[I17Y]: G E γ γ **Y**^{5} A K M A A^{10} **A** L A R **A** ^{15} N **Y**-NH$_2$

All variant peptides have been previously assayed for NMDAR activity and display inhibitory potencies comparable to their wild-type counterparts (refs *16* and *17* and Q. Dai, unpublished observations)

Iodination of Conantokins. Con-T, Con-G/Ala[A16Y], and Con-G[S16Y] were radiolabeled with ^{125}I using chloramine-T (Acros Organics, Morris Plains, NJ). Briefly, 1 μL of a 100 mM aqueous solution of chloramine-T was added to 200 μL of a solution containing ca. 0.5 mg of peptide and 1 mCi of Na^{125}I (ICN, Irvine, CA) in 100 mM sodium phosphate buffer (pH 7.4). The reaction was allowed to proceed for 2 min before being quenched by the addition of 6 μL of 1 M $Na_2S_2O_5$. The mixture was diluted with 300 μL of H_2O and loaded onto a C-18 SEP-PAK cartridge column (Waters Associates, Inc., Milford, MA) preequilibrated with 5% acetonitrile. The column was washed with 6 mL of 5% acetonitrile, followed by elution of peptide with 6 mL of 60% acetonitrile. Collected fractions (0.5 mL) were counted on a γ-counter. Fractions corresponding to peptide were pooled and lyophilized. When necessary, further separation of free ^{125}I from the peptide-incorporated label was accomplished by HPLC using a Vydac C_{18} column (218TP 4.6 × 250 mm), equilibrated in 95:5 (v/v) 0.1% TFA/0.1%TFA/CH_3CN at a flow rate of 1.0 mL/min. At a time of 3 min postinjection, a 40 min linear gradient was applied to a limiting value of 60:40 (v/v) 0.1% TFA/0.1% TFA/CH_3CN. Absorbance detection was performed at 214 nm. Individual fractions were γ-counted.

PL Preparations. Small unilamellar vesicles were prepared as described previously (*18*). PLs (10−14 mg) were resuspended in 1−3 mL of buffer (10 mM sodium borate/100 mM NaCl, pH 6.5) with gentle swirling and purged under N_2 for 5 min. The dispersions were pulse sonicated at 4 °C under N_2, using a Heat Systems Model W200R sonicator (Farmingdale, NY) equipped with a standard microtip probe adjusted to deliver a power output of 45 W on a 50% duty cycle. After a sonication time of 15 min, the clarified suspensions were centrifuged for 1 h at 200 000*g*, and the supernate was collected. The PL concentrations of these stock vesicle solutions were determined by phosphorus analysis (*19*). All vesicle solutions were used within 48 h after preparation.

The preparation of oriented peptide-PL multilayers was based on described procedures with some modifications (*20*−*22*). Peptide and PLs were codissolved in methanol/H_2O (4:1 v/v) at concentrations of 10 mg/mL lipid (∼12.5 mM) and an amount of peptide to achieve a peptide/PL mole ratio of 1:25 or 1:60. A 15 μL (1:25 preparation) or 25 μL (1:60 preparation) aliquot of the stock solution was deposited onto a 7 × 25 mm area in the center of a window of a 1 cm quartz cuvette. Solvents were removed under vacuum, and the cuvettes were mounted in a sealed container over 1 M NaCl. They were allowed to hydrate for 2∼3 days until the multilayer films became transparent. The preparation of each sample was repeated three times. The homeotropic alignment of PL multiplayers was confirmed by the method of conoscopy (*23*) and atomic force microscopy (AFM) using a Digital Instruments Multimode Nanoscope III A (Santa Barbara, CA).

Binding Assays. Nonequilibrium binding analyses were performed using size-exclusion chromatography on either a Sephadex G-25 superfine column (1 × 28 cm) and/or a Bio-Sil SEC 250-5 (300 × 7.8 mm) HPLC column (Bio-Rad Laboratories). Radioiodinated conantokins (20−35 pmol, 1.3−2.3 Ci/mmol) were incubated with and without vesicles (1 mg) in 0.5 mL of 10 mM sodium borate/100 mM NaCl, pH 6.5 for 15 min at 4 °C. Mixtures were applied to the Sephadex G-25 column equilibrated with either 5 mM Ca^{2+} or 2 mM EGTA in 10 mM sodium borate/100 mM NaCl (pH 6.5) and eluted at 0.2 mL/min. PL vesicle-containing fractions were identified by light scattering at 320 nm. Radioactivity was determined using a γ-counter. Using HPLC, the concentration of conantokins and the total amount

of vesicle were the same as that in Sephadex G-25 analyses.

Circular Dichroism. Solution and oriented CD spectra were recorded between 190 and 260 nm on an AVIV Model 202SF spectrometer maintained at 25 °C. For solution CD, quartz cells of either 1, 0.2, or 0.02 cm path length were used. The buffer was 10 mM sodium borate/100 mM NaCl, pH 6.5. The α-helical content of peptides in solution was determined from the mean residue ellipticities at 222 nm using the empirical relationship, $\text{fraction}_{\text{helix}} = (-[\theta]_{222} - 2340)/30300$ (*24*). Each solution and oriented CD spectrum represents the average of three scans collected at 1.0 nm intervals at a 1.0 nm bandwidth. In both techniques, corrections for nonpeptidic contributions to the ellipticity were made by subtracting the averaged spectrum of the peptide-free sample. For oriented CD, the optical axis was normal to the peptide-PL film on the quartz cuvette.

Fluorescence. Fluorescence measurements were made on a SLM-Aminco 8100 steady-state recording spectrofluorimeter (SLM-Aminco Instruments, Urbana, IL), using slit widths of 2 nm (excitation) and 4 nm (emission). All measurements were performed in 10 mm path length semimicro quartz cuvettes at room temperature. To correct for polarization effects and reduce contributions from vesicle scattering, the excitation polarization was set to 54.7°, while emission polarization was set to vertical. Excitation wavelengths of 270 and 300 nm were used to excite tyrosine and tryptophan, respectively. Peptide concentrations of 10 and 2 μM were employed for tyrosine- and tryptophan-containing peptides, respectively, in 10 mM sodium borate/100 mM NaCl, pH 6.5. In all cases, the background fluorescence spectra, corresponding to vesicles in buffer, were recorded and subtracted from the peptide-containing sample. Acrylamide quenching measurements were performed by titrating a freshly prepared 4 M solution of acrylamide into peptide-PL suspensions and recording the fluorescence intensity at 305 nm (for tyrosine, N^{α}-Ac-tyrosine and tyrosine-containing peptides) or at 350 nm (for tryptophan, N^{α}-Ac-tryptophan and tryptophan-containing peptides). The quenching constants K_{sv} were obtained by linear regression with the equation $F_0/(F_0 - F) = 1/f_1 + 1/(f_1 K_{sv}[Q])$, where F and F_0 are the fluorescence intensities in the presence and absence of the quencher (Q), respectively, and f_1 is the initial fraction of the fluorescence that is accessible to the quencher (i.e., the ratio of the K_{sv} of the peptide in buffer to the K_{sv} of N^{α}-Ac-tyrptophan (or N^{α}-Ac-tyrosine) in buffer (*25*)). Fluorescence intensities were corrected for dilution and light scatter.

NMR Spectroscopy. Vesicle-peptide samples for NMR measurements were prepared in 10 mM sodium borate/100 mM NaCl (pH 6.5), 6% D_2O, 10 μM EDTA, and 25 μM DSS as internal standard (^{1}H $\delta = 0$ ppm). The final concentration of peptide was 1 mM, while vesicle concentrations (DMPS and DMPC/DMPS (80:20); DMPS-d_{54} and DMPC-d_{54}/DMPS-d_{54} (80:20)) were 25 mM. Because of the high concentration of vesicles required, the vesicle solutions were centrifuged for 20 min at 22 000*g*. All NMR experiments were carried out at 20 or 30 °C on a Varian INOVA spectrometer operating at 11.7 T (499.87 MHz, ^{1}H). An inverse detection triple-resonance probe with *xyz* gradients was used for 2-D DQF-COSY, TOCSY, and NOESY experiments employing standard pulse sequences (*26*, *27*) and a States−Haberkorn phase cycling scheme (*28*). The solvent signal was suppressed by selective presaturation during the relaxation delay. The relaxation delays of 1.6 s were used for the DQF-COSY and TOCSY experiments and 3.8 s for the NOESY experiments. Mixing times were 65 ms for TOCSY and 150−250 ms for NOESY. All 2-D spectra were recorded with the spectral width of 5400 Hz in both F_1 and F_2 frequency domains, as 2048 × 256 time domain (t_2, t_1) complex point matrixes with 64−80 scans per t_1 increment. Time domain data were linearly predicted to the 512 t_1 complex points, zero filled in both domains to a final (t_2, t_1) matrix of 4096 × 2048 and apodized with Gaussian weighting functions prior to Fourier transformation. A first-order baseline correction was applied in the F_2 domain. A broadband probe was employed for ^{13}C T_1 and T_2 measurements on ^{13}C-labeled con-G/Ala using inversion recovery (*29*) and CPMG techniques (*30*), respectively. Both measurements were carried out with proton broadband decoupling. Fourteen different τ values were used to define the T_1 and T_2 relaxation curves, and the corresponding relaxation delays were 7 and 5 s, respectively. The T_1 and T_2 values were obtained from three parameter fits to the raw data (*31*). All NMR spectra were processed using Varian VNMR software.

Amide Proton Exchange Rates. Aqueous peptide solutions containing EDTA and DSS were lyophilized and redissolved in water. The solutions were neutralized to pH 6.5 with dilute NaOH and lyophilized again. The resulting solids were dissolved in D_2O buffer (10 mM borate sodium/100 mM NaCl, pH 6.5) containing 25 mM sonicated DMPC-d_{54}/DMPS-d_{54} (80:20) and immediately monitored for disappearance of ^{1}H-amide proton resonances by measuring 1-D ^{1}H spectra. (The final concentrations of peptide, EDTA, and DSS are the same as for NOESY and TOCSY experiments.) Data were acquired on a 500 MHz Varian Inova spectrometer using a 60° pulse at a 5500 Hz spectral width in 8000 complex data points. Each spectrum was a sum of 64 transients.

RESULTS

Binding to PL Vesicles. The binding of trace radioiodinated conantokins including con-T, con-G[S16Y], and con-G/Ala-[A16Y] (an alanine-rich con-G analogue with high biological activity (*16*)) to vesicles under nonequilibrium conditions was determined by high-performance size-exclusion chromatography. A representative analysis is shown in Figure 1, and the data are summarized in Table 1. Among the four kinds of vesicles examined, the three conantokins all bound to BLPC to a greater degree than to mixed vesicles, suggesting that conantokins preferentially bind to zwitterionic vesicles. Both spermine and Ca^{2+} slightly increased the binding. As compared to other conantokins tested, con-G/Ala[A16Y] displayed the highest binding ability. The binding ratio of con-G/Ala[A16Y] to BLPC/DOPC (50:50) is 2.0 and 2.5% in the absence or presence of 5 mM $CaCl_2$, respectively. Hence, the presence of di-oleyl chains does not contribute appreciably to the decrease in peptide binding observed with BLPC/DOPS or BLPC/DOPG vesicles. The decrease in binding can therefore be attributed to a reduced preference for acidic vesicles. Incubation of $Na^{125}I$ with vesicles did not result in any coelution of radioactivity with vesicles, indicating that all vesicle-associated radioactivity can be attributed to peptide rather than free ^{125}I.

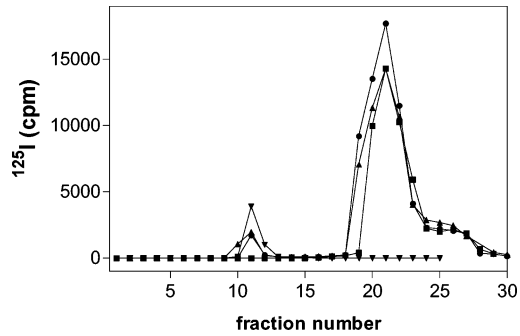

FIGURE 1: Nonequilibrium binding of [^{125}I]con-G/Ala[A16Y] to PL vesicles determined by high-performance size-exclusion chromatography. Radioiodinated con-G/Ala[A16Y] (20 pmol) was incubated with and without BLPC vesicles (1 mg) in 10 mM sodium borate/100 mM NaCl, pH 6.5 for 15 min at 4 °C. Mixtures were analyzed by injection onto a Bio-Sil SEC 250 column (300 × 7.8 mm) equilibrated with either 5 mM $CaCl_2$ or 2 mM EGTA, in 10 mM sodium borate/100 mM NaCl, and eluted at 0.5 mL/min. Fractions corresponding to 0.5 mL were collected. Vesicles eluted at the void volume (5.2 mL). Peptide and 5 mM $CaCl_2$ (■); peptide and BLPC (●); peptide, BLPC, and 5 mM $CaCl_2$ (▲); and relative value of light scattering (▼).

Table 1: Radiolabeled Conantokin Binding to Neutral and Acidic Vesicles (% of Total Radioactivity)

conditions[a]	con-G/Ala[A16Y]	con-G[S16Y]	con-T
BLPC	2.6	1.1	1.2
BLPC + 5 mM Ca^{2+}	3.2	1.6	1.8
BLPC + 1 mM spermine	2.9	1.2	1.9
BLPC/DOPS	0.6	0.3	0.6
BLPC/DOPS + 5 mM Ca^{2+}	0.9	0.4	0.8
BLPC/DOPS + 1 mM spermine	1.0	0.5	1.3
BLPC/DOPG	0.4	0.1	0.2
BLPC/DOPG + 5 mM Ca^{2+}	0.5	0.3	0.3
BLPC/DOPG + 1 mM spermine	0.5	0.4	1.0
BLPC/DOPC	2.0		
BLPC/DOPC + 5mM Ca^{2+}	2.5		

[a] A 1 mg vesicle, BLPC/DOPC (50:50), BLPC/DOPS (80:20), and BLPC/DOPG (50:50). The reported % binding values represent the average binding determined from two separate incubations and did not deviate by more than 10% between duplicate experiments. Values were determined based on the total cpm of all fractions coeluting with vesicles as compared with the total cpm of the injected sample.

Conantokin Fluorescence Emission in the Presence of PL Vesicles and Fluorophore Quenching by Acrylamide. The only aromatic amino acid that is native to the conantokins is a tyrosine that occurs at position 5 of con-T. Tyrosine is a weak fluorophore and displays spectral properties that are relatively insensitive to the local environment, although deprotonation of the tyrosine hydroxyl can result in a slight (~5 nm) red-shift in emission maximum as well as the self-quenching of fluorescence (*32*, *33*). Tryptophan, on the other hand, has a much higher quantum yield, and its fluorescence spectrum is highly sensitive to the polarity of the environment. Intrinsic tryptophan fluorescence has been widely implemented to monitor and report the interaction of peptides and proteins with membranes (*32*, *34*). Hence, to augment fluorescence sensitivity for the purposes of determining conantokin accessibility to the hydrophobic region of the membrane, two tryptophan-containing conantokin analogues, con-T[Y5W] and con-T[K7W], were also examined. In

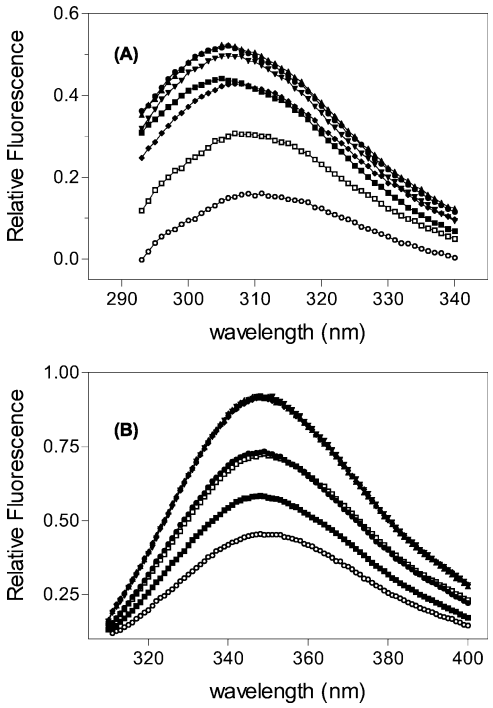

FIGURE 2: Effects of vesicle concentration on fluorescence spectra of the designated conantokins. Excitation at 270 and 300 nm was used to excite tyrosine (con-G[A16Y]) and tryptophan (con-T[Y5W], con-T[K7W]), respectively. (A) Con-G[A16Y]) and (B) con-T[Y5W]. Con-G and con-T[K5W] were dissolved in DOPC vesicles at the following vesicle concentrations: 0 mM (■), 0.008 mM (●), 0.04 mM (▲), 0.08 mM (▼), 0.16 mM (◆), 0.4 mM (□), and 0.8 mM (○).

general, we found that the fluorescence emission spectra of conantokins and their variants displayed highly changeable tendencies in the presence of increasing concentrations of PL vesicles. Figure 2 depicts a series of fluorescence emission spectra of con-G/Ala[A16Y] and con-T[Y5W] acquired at varying DOPC vesicle concentrations. The intensities of both tyrosine and tryptophan fluorescence emission signals initially increase with initial vesicle concentrations as low as 8 μM, then decrease at a higher concentration of vesicles. For the tryptophan-containing peptides examined, the λ_{max} of emission remained unchanged with increasing vesicle concentration, whereas a small red-shift (3−5 nm) was observed for all tyrosine-containing peptides. The introduction of 5 mM $CaCl_2$ had no effect on the fluorescence spectra with any of the conantokins, nor were different trends observed in with BLPC or with acidic PLs present (data not shown). The position of tyrosine or tryptophan within the peptide sequence (i.e., con-G[S16Y], con-G/Ala[A16Y], con-R17/Ala[I16Y], con-R[V5Y], con-T, con-T[Y5W], and con-T[K7W]) had no effect on this tendency.

Aqueous exposure of tryptophan and tyrosine residues in the presence of vesicles was further characterized by acrylamide quenching experiments. Acrylamide is a nonionic, aqueous phase fluorophore quencher. It does not interact with peptides, and unlike iodide, is not influenced by nearby charged residues (*32*). Hence, the value of the Stern−Volmer constant, K_{sv}, for the acrylamide quenching of tryptophan and tyrosine provides an estimate of the relative exposure of these residues to the aqueous phase. Plots of F_0/F versus [Q] manifested upward deviations from linearity for tyrosine-containing conantokins and downward trends for tryptophan-

Table 2: Exposure of Tryptophan and Tyrosine in Conantokins to Acrylamide (K_{sv} (M^{-1}))

conantokins oramino acids	buffer[a]	BLPC[b]	DOPC[c]	DOPC/DOPS
con-T	22.2 ± 3.5	16.6 ± 1.4	17.8 ± 1.5	19.1 ± 3.7
con-T + Ca^{2+} [d]	24.0 ± 3.5	18.4 ± 2.2	15.9 ± 2.1 7	20.5 ± 2.7
con-T[Y5W]	19.8 ± 2.0	13.5 ± 2.5		
con-T[Y5W] + Ca^{2+}	14.8 ± 1.9	15.1 ± 1.9		
con-T[K7W]	10.2 ± 1.0	8.6 ± 1.0, 6.5 ± 1.1[e]		
con-T[K7W] + Ca^{2+}	10.7 ± 1.2	8.9 ± 1.2		
con-G/Ala[A16Y]	24.0 ± 1.5	22.9 ± 1.5	20.2 ± 1.4	15.9 ± 2.3
con-G/Ala[A16Y] + Ca^{2+}	24.1 ± 1.3	19.4 ± 1.5	22.6 ± 1.7	15.0 ± 2.5
con-G[S16Y]	21.2 ± 2.5	17.1 ± 2.0	20.9 ± 1.8	16.8 ± 1.9
con-G[S16Y] + Ca^{2+}	22.3 ± 2.7	20.1 ± 3.3	20.4 ± 2.1	14.5 ± 2.6
con-R17/Ala[I17Y]	23.5 ± 2.7	20.8 ± 2.0	17.9 ± 2.2	18.0 ± 1.3
con-R17/Ala[I17Y] + Ca^{2+}	26.0 ± 3.0	16.5 ± 2.2	17.6 ± 1.5	20.7 ± 2.5
con-R17[V5Y]	21.1 ± 2.0		20.9 ± 1.9	20.3 ± 1.6
con-R17[V5Y] + Ca^{2+}	22.2 ± 2.5		19.9 ± 1.4	19.5 ± 2.1
N^{α}-Ac -tyrosine	28.1 ± 3.7			
N^{α}-Ac -tryptophan	20.4 ± 1.9			

[a] Buffer was 10 mM sodium borate/100 mM NaCl, pH 6.5. [b] At 0.9 mM BLPC. [c] At 1.5 mM DOPC, DOPC/DOPS (80:20). [d] Buffer included 5 mM $CaCl_2$. [e] At 1.5 mM BLPC.

containing conantokins in either the presence or the absence of the vesicle, leading to a poor fit of the data using Stern−Volmer calculations ($F_0/F = (1 + K_{sv}[Q])(1 + K_a[Q])$ or $F_0/F = (1 + K_{sv}[Q])\exp(V[Q])$). Such slightly curved Stern−Volmer plots are indicative of the presence of a population of inaccessible fluorophores or of structural heterogeneity. Because more than one conformation of conantokin exists in solution (random coil vs helix), tryptophan and tyrosines contained therein could be less accessible in the structured peptide. Instead, the modified Stern−Volmer equation ($F_0/(F_0 - F) = 1/f_1 + 1/(f_1K_{sv}[Q])$) introduced by Lehrer and Leavis (*25*) for nonlinear Stern−Volmer plots was used to analyze the data. Excellent linear fits ($r^2 \geq 0.98$) and good reproducibility were obtained. The quenching constants are summarized in Table 2. In general, the quenching constants of conantokins in all vesicles tested decreased by as much as 37% in comparison with those in buffer, suggesting that the exposure of tryptophan and tyrosine to water decreases to some extent in the presence of the bilayers.

Effects of PL Vesicles and Aligned Multilayers on the Ellipticity and Orientation of Conantokins. The well-documented Ca^{2+}-induced helical conformations of con-T and con-G (*14*, *35*) are not greatly changed by the presence of PL vesicles as shown with BLPC vesicles in Figure 3. Similar results were obtained for vesicles comprised of DOPC and DOPC/DOPS (80:20) as well as for con-R17 (data not shown). However, in the absence of Ca^{2+}, increased vesicle concentration exerts a positive effect on the secondary structure of con-G, effecting a change from 4 to 15% helical content. No vesicle effects on helicity were noted with con-T and con-R17 (data not shown) in their apo forms.

We also examined the CD spectra of the conantokins in aligned PL membrane films. The approach, referred to as oriented CD, provides an indication of the directional state of helical peptides relative to aligned membrane films (*22*, *23*). The method assumes that the helical peptide axis can orient in either a parallel or a perpendicular manner with respect to the optical light path. Empirically, when compared with the isotropic solution CD spectrum, a decrease in the intensity of the 207 nm band relative to the absorbance at 222−228 nm is diagnostic of a peptide population for which the helix is perpendicular to the membrane surface (i.e., parallel to the incident light beam). The opposite is observed when the helix axis is parallel to the membrane surface (normal to the incident light beam). Confirmation of the multilayer nature of the PL films as generated in our hands was achieved by AFM. Most of the multilayer surface was uniformly smooth, although small pits were observed. An AFM image of a pitted area clearly shows the existence of a multilayer organization (Figure 4). The ordered alignment of all PL multilayers was verified through conoscopy, in which interference patterns consistent with anisotropic formats were observed (*23*) (data not shown). The solution CD of the apo conantokins in the presence of DOPC vesicles is shown in Figure 5A. Similar spectra were obtained with BLPC and mixed vesicle systems (data not shown). The oriented CD spectra of conantokins in different aligned membrane multilayers are shown in Figure 5B−E (Ca^{2+} was not included in these experiments since precipitation leading to impracticable amounts of light scattering was observed in all peptide-PL films generated in the presence of Ca^{2+}). In BLPC films, the conantokins appear to orient perpendicularly to the membrane film (Figure 5B). For other membrane compositions (Figure 5C−E), the perpendicular component

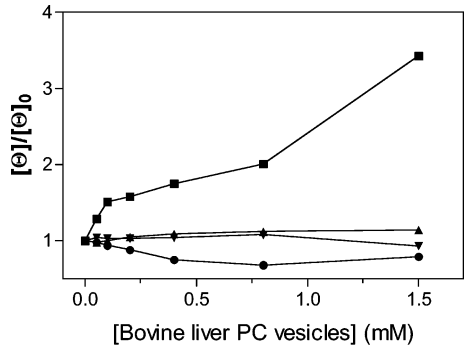

FIGURE 3: Effects of the concentration of BLPC vesicles on the relative ellipticities of con-G and con-T (35 μM) in the presence and absence of Ca^{2+}. Ellipticity ratios were derived from the average of three CD measurements at 222 nm. Spectra were recorded at 25 °C in 10 mM sodium borate/100 mM NaCl, pH 6.5 using a 0.2 cm path length cell. Corrections for nonpeptidic contributions to the ellipticity at 222 nm were made by subtracting the average of three readings of the peptide-free sample. Con-G (■), con-G in 5 mM Ca^{2+}(●), con-T (▲), and con-T in 5 mM Ca^{2+} (▼).

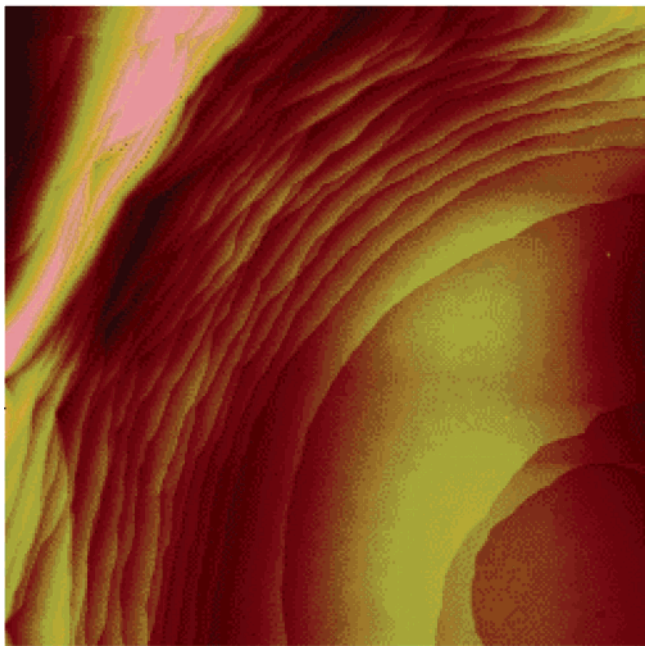

FIGURE 4: AFM image of the multilayer structure in the interior of a small pit in DOPC multilayers. Scan size was 15.46 × 15.46 μm. Image was collected in tapping mode at a scan rate of 1 Hz.

decreases, particularly in DOPC/DOPS and DOPC/DOPG multilayers. Also, in these latter multilayers, con-R17 displays a distinct preference for parallel partitioning to the membrane. Spectra collected at a higher ratio of lipid to peptide (60:1) were qualitatively similar to those presented in Figure 5 (lipid/peptide 25:1).

NMR Spectra in the Presence of Vesicles. NMR has been widely used to determine the structure of peptides in micelles and vesicles (reviewed in refs *36* and *37*), but there have been few successful attempts to ascertain the binding mode of peptides (*38*−*40*) or drugs (*41*) to PLs in solution. By employing vesicles comprised of lipids with fully deuterated acyl chains, we examined chemical shift deviations and monitored deuterium−proton exchange to identify con-G/Ala, con-G, and con-T residues involved in contacts with vesicles. We also measured peptide−lipid NOEs with fully protonated vesicles. Additionally, we synthesized a ^{13}C-labeled analogue of con-G/Ala, with ^{13}C incorporated at a selected backbone carbonyl and side-chain carbons. The mobility of the labeled carbons was evaluated through the measurements of T_1 and T_2 relaxation times in the presence and absence of vesicles. The selection of con-G/Ala for this study was governed by its higher vesicle binding ability as compared to other conantokins (Table 1). These studies necessitated sequence-specific proton and ^{13}C assignments of con-G/Ala and are summarized in Table 3. When vesicles (DMPS-d_{54}, DMPC-d_{54}/DMPS-d_{54} (50:50), and DMPC-d_{54}/DMPS-d_{54} (80:20)) are present in the solutions, the values of ^{1}H and ^{13}C chemical shifts change only slightly (0−0.12 ppm, ^{1}H; 0−0.2 ppm, ^{13}C). For instance, in DMPS-d_{54} vesicles versus buffer, all 16 backbone NH protons of con-G/Ala exhibited upfield chemical shifts (−0.02 to −0.11 ppm), while all αCH protons shifted slightly downfield (0.06−0.11 ppm). The proton chemical shift assignments of con-G and con-T in the same buffer conditions were previously reported (*42*, *43*). They also exhibit only minor changes (0∼0.1 ppm) in the presence of the indicated deuterated vesicles.

In solution studies with fully protonated DMPC/DMPS vesicles, we did not observe any NOEs among the NH and αCH protons of con-G/Ala, con-G, and con-T and the fatty acid methylene (1.26 ppm) and methyl protons (0.89 ppm) of the PLs. However, strong NOEs between the PL headgroups and the αCH and side-chain protons of the peptides were detected. Weak NOEs between peptide NH protons and PL headgroup protons were also noted. Some typical NOESY spectra for these regions are shown in Figure 6.

For con-G/Ala, residues Gla^4, Gly^6, Lys^7, Ala^{10}, and Ile^{12} were unambiguously identified in binding to the $N(CH_3)_3^+$ and CH_2N^+ moieties of DMPC. Simultaneously, no binding between the con-G/Ala residues and the serine headgroup of DMPS was observed. In the case of con-G, several peptide residues appear to contact the DMPC headgroup in the presence of DMPC/DMPS vesicles. In particular, Gla^4, Leu^{11}, Arg^{13}, Lys^{15}, and Asn^{17} are implicated in extensive vesicle interaction, as evidenced by the strong NOE contacts among the amide, αCH, and side-chain protons of the aforementioned residues with the DMPC headgroup. As for con-T, residues Gla^4, Tyr^5, Lys^7, Met^8, Leu^9, Arg^{13}, Val^{17}, Lys^{18}, Asn^{20}, and Ala^{21} appear to be involved in the binding to the polar bilayer surface. In the presence of 5 mM Ca^{2+}, the binding of con-T and con-G/Ala to DMPC/DMPS vesicles was similar to that described for the Ca^{2+}-free experiments.

Amide Proton Exchange Rate. Con-G/Ala in aqueous solution or in DMPC-d_{54}/DMPS-d_{54} (80:20) exhibits no protected proton resonances, as no amide proton signals were observed after the 4 min dead time associated with the experiment. Con-T exhibits some backbone amide protection for Lys^{18}, Leu^{12}, and Leu^9, but the lifetimes are short (≥8 min) in both buffer and DMPC-d_{54}/DMPS-d_{54} (80:20). This further demonstrates that conantokins tested are not embedded beyond the surface of DMPC-d_{54}/DMPS-d_{54}.

Mobility of Con-G/Ala in Solutions and Solutions Containing Vesicles. The relaxation times, T_1 and T_2, of ^{13}C-labeled backbone carbonyl carbons or ^{15}N-labeled amides of the peptide reflect both the internal and the overall molecular mobility (*39*, *40*). Possible differences in the backbone mobility of con-G/Ala in solutions and DMPC/DMPS vesicles were evaluated by measuring T_1 and T_2 of the labeled ^{13}C-carbonyl carbons at selected positions (Table 3). The results are summarized in Table 4. Upon introduction of DMPC/DMPS vesicles into solution, the values of T_1 and T_2 are the same within the experimental error, except for T_1 for Gly^1 and T_2 for Gly^6 and Ala^{10}. These values decreased in the presence of DMPC/DMPS, suggesting a slight restriction in backbone mobility of these residues.

DISCUSSION

Using size-exclusion chromatography under nonequilibrium conditions, the binding of radiolabeled conantokins to PL vesicles has been demonstrated (Figure 1 and Table 1). While only small percentages (≥3.2%) of the total amount of introduced radioiodinated peptides bound to vesicles (Table 1), these are not unexpected under nonequilibrium conditions. Previous work employing similar types of gel-filtration experiments to ascertain the membrane-binding

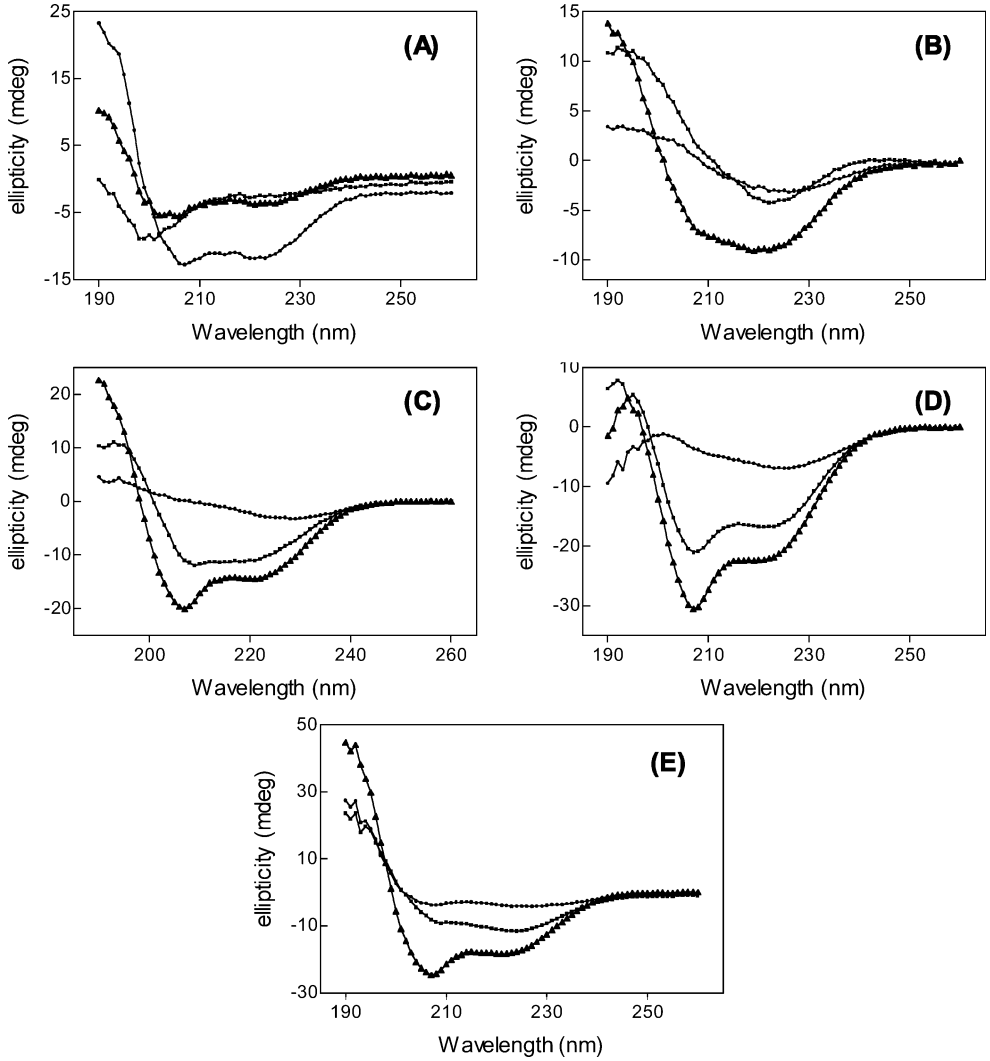

FIGURE 5: Solution and oriented CD of conantokins in the presence of PL vesicles or multilayers. Peptide/PL, 1:25. (A) Solution CD in DOPC; (B) oriented CD in BLPC; (C) oriented CD in DOPC; (D) oriented CD in DOPC/DOPS (50:50); and (E) oriented CD in DOPC/DOPG (50:50). Con-G (■), con-R17 (▲), and con-T(●).

affinity of vitamin K-dependent blood proteins has shown that low percentages of the radiolabeled protein pools (ca. 20%) migrate with PL vesicles despite the high affinities of these protein/vesicle interactions (K_d values ca. 0.25−15 μM) (*10*, *44*, *45*). Slight increases in conantokin binding to both neutral (BLPC) and acidic (BLPC/DOPS) vesicles were noted in the presence of Ca^{2+} and spermine. These vesicle-binding properties are in contrast to the behavior of the vitamin K-dependent blood proteins, which bind exclusively to negatively charged PL surfaces in a Ca^{2+}-dependent manner (*8*−*11*). It is generally recognized that this translocation involves electrostatic interactions between the Ca^{2+}-complexed carboxylate moiteies of Gla residues located in the N-terminal domain and the negatively charged phosphatidylserine headgroups, although hydrophobic interactions may account for a portion of the binding energy (*11*, *46*). Because the conantokins bind to neutral membranes to a greater extent than to acidic membranes, and can do so in the absence of Ca^{2+} or spermine, the involvement of Gla residues in vesicle adhesion may be minimal. Further underscoring this possibility is the following order of binding affinity: con-G/Ala (two Gla residues, net charge of −2) > con-T (four Gla residues, net charge of −5) > con-G (five Gla residues, net charge of −8). Hence, while electrostatics may be mediating a portion of conantokin binding, they are not the principal forces underlying peptide−vesicle interaction. In fact, a high negative charge appears detrimental to vesicle binding, particularly in the case of anionic bilayers, wherein peptide−vesicle charge repulsion would be expected to prevail. As such, the higher binding ability of con-G/Ala-[A16Y] may be attributed to its higher hydrophobicity.

The fluorescence emission spectra collected with an array of conantokins at varying vesicle concentrations, for which representative data are shown in Figure 2, revealed an increase in fluorescence intensity at lower (8 μM) vesicle concentrations and a reduction in the relative intensity at higher concentrations. The highly variable nature of the intrinsic tyrosine or tryptophan fluorescence with vesicle concentration did not allow for the straightforward determination of an EC_{50} for vesicles for either fluorescence increasing or fluorescence decreasing transitions. The photophysics of both tryptophan and tyrosine in these systems is clearly complex, with numerous inter- and intramolecular interactions likely contributing to the variability in quantum yield. The absence of a blue-shift in the λ_{max} of emission for tryptophan-containing peptides indicates that no embedding of these

Table 3: Proton and ^{13}C Resonance Assignments of Con-G/Ala[a]

residue	chemical shift (ppm)				
	^{13}C[b]	NH	αH	βH	other H
Gly[1]	171.41	3.64, 3.58			
Glu[2]		9.07	4.19	2.09, 2.00	2.30, 2.00(γCH_2)
Gla[3]	180.82, 180.60	9.19	4.13	2.20	3.14, 2.98(γCH)
Gla[4]	180.89, 180.38	8.28	4.06	2.25	3.18, 3.22(γCH)
Leu[5]	179.12	8.03	4.17	1.72	1.62(γCH_2), 0.95, 0.90(δCH_3)
Gly[6]	176.01	8.34	3.91		
Lys[7]		7.85	4.13	1.85, 1.65	1.70(γCH_2), 1.53(δCH_3), 2.97(ϵCH_2), 7.78(ϵNH_3^+)
Ala[8]	179.63	8.09	4.16	1.48	
Gln[9]		8.25	4.10	2.12, 2.09	2.48, 2.44 (γCH_2), 6.91, 7.53(δNH_2)
Ala[10]	179.18	8.07	4.13	1.44	
Leu[11]	178.65	7.89	4.17	1.76	1.59(γCH), 0.94, 0.90(δCH)
Ile1[12]		7.89	3.94	1.90	1.58, 1.25(γCH_2), 0.93(γCH_3), 0.89 (δCH_3)
Arg[13]		8.19	4.17	1.83, 1.72	1.62(γCH_2), 3.25, 3.20(δCH_2), 7.28(ϵNH)
Ala[14]	178.42	8.13	4.19	1.43	
Ala[15]		8.05	4.19	1.43	
Ala[16]		8.02	4.19	1.41	
Ala[17]		8.02	4.19	1.41	7.41, 7.08(NH_2)

[a] Measurements were carried out in 10 mM $NaBO_3$/100 mM NaCl, pH 6.5, 20 °C. Peptide concentration was 1 mM. [b] Carbonyl carbon of G^1, L^5, G^6, A^8, A^{10}, L^{11}, and A^{14}, as well as two carbonyl carbons of Gla^3 and Gla^4 in the side chain, are ^{13}C labeled.

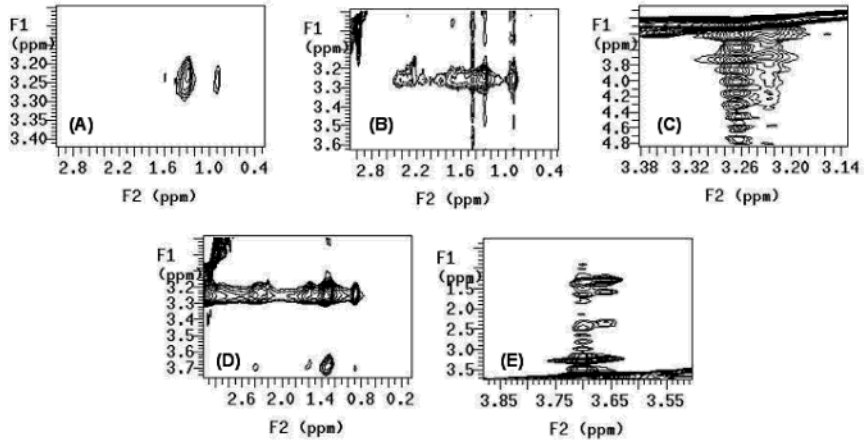

FIGURE 6: NOEs between side chain or αCH of conantokins (1 mM) and the PC headgroup DMPC in a mixed vesicle solution (DMPC/DMPS, 80:20, 25 mM). The resonance at 3.25 ppm is assigned to the cholinemethyl groups ($-N(CH_3)_3^+$) of DMPC; 3.66∼3.71 ppm is assigned to CH_2N- of DMPC. (A) DMPC/DMPS; (B and C) con-G/Ala in DMPC/DMPS; and (D and E) con-T in DMPC/DMPS.

peptides into the hydrophobic core of the bilayer is occurring. Generally, a tryptophan side chain that is completely or partially buried in the hydrophobic core of the lipid bilayer results in a 5−25 nm blue-shift in the emission maximum (*47*). This suggests a model for conantokin involvement with the vesicle bilayer that involves partitioning of the peptide parallel to the membrane surface. Further evidence for this is provided by the slight red-shift in the emission spectra observed for all tyrosine-containing conantokins. Red-shifts of this type have been attributed to deprotonation of the tyrosine hydroxyl group (*34*), suggesting possible contact of the tyrosine side chain with the monoanionic phosphodiester headgroups of the lipid surface.

The acrylamide quenching studies further demonstrate that tryptophan and tyrosine residues in the conantokins are localized at a hydrated region of the membrane rather than in the hydrophobic core. Stern−Volmer constants for both amino acids were decreased slightly (≥37%) in the presence of vesicles, regardless of their relative placement in the conantokin primary sequence (i.e., at positions 5, 7, 16, and 17). In the heptad repeat representation of an α-helix, these specific residues would occupy positions e, g, b, and c, respectively (residue 1 is assigned as a). Hence, no particular face of the helix is preferentially bound to the vesicle surface. Furthermore, no significant differences in fluorophore accessibility were noted between the neutral and the acidic vesicles. The presence of Ca^{2+} and its ability to impart increased helicity to the conantokins was also without effect on the quenching constants. This suggests a model of rapid association and dissociation from the membrane surface that is independent of Ca^{2+}-induced helical content.

The effect of increasing vesicle concentration on the helical character of the conantokins in solution was minimal for the apo forms of con-T and con-R17 as well as the Ca^{2+}-

Table 4: Relaxation Times (s) of ^{13}C-Labeled Residues of Con-G/Ala in Aqueous Solution and DMPC/DMPS

^{13}C-labeled residues	con-G/Ala[a]		con-G/Ala + DMPC/DMPS[b]	
	T_1	T_2	T_1	T_2
Gly^1	1.411 ± 0.111	0.281 ± 0.065	1.213 ± 0.063	0.296 ± 0.062
Gla^3	1.908 ± 0.077	0.431 ± 0.079	2.076 ± 0.076	0.457 ± 0.102
Gla$^{3'}$	2.210 ± 0.081	0.374 ± 0.140	2.151 ± 0.057	0.492 ± 0.175
Gla^4	2.106 ± 0.084	0.065 ± 0.021	2.096 ± 0.061	0.091 ± 0.018
Gla$^{4'}$	2.185 ± 0.064	0.077 ± 0.020	2.106 ± 0.093	0.096 ± 0.020
Leu^5	1.011 ± 0.024	0.461 ± 0.058	0.953 ± 0.029	0.380 ± 0.063
Gly^6	1.064 ± 0.024	0.513 ± 0.100	1.010 ± 0.029	0.314 ± 0.027
Ala^8	1.068 ± 0.040	0.278 ± 0.046	1.112 ± 0.035	0.397 ± 0.072
Ala^{10}	1.091 ± 0.037	0.302 ± 0.029	1.094 ± 0.039	0.198 ± 0.027
Leu^{11}	1.037 ± 0.034	0.290 ± 0.033	1.029 ± 0.047	0.297 ± 0.030
A1a^4	1.255 ± 0.036	0.379 ± 0.056	1.221 ± 0.047	0.493 ± 0.082

[a] Con-G/Ala concentration was 1 mM in 10 mM sodium borate/100 mM NaCl. [b] DMPC/DMPS (80:20) concentration was 37 mM.

complexed forms of con-G, con-T, and con-R17. However, increasing vesicle concentration had a profound effect on the helicity of apo con-G (Figure 3). Whereas con-T and con-R17 manifest considerable helical content in the absence of divalent metal cations (55 and 23%, respectively) (*14*, *48*), con-G is essentially structureless under metal-free conditions owing to a preponderance of charge repulsion occurring among Gla residues occupying sequence positions *i*, *i* + *3* and *i*, *i* + *4* (*42*). That helical content is unchanged for all Ca^{2+}-complexed peptides upon the addition of vesicles, suggesting that Ca^{2+} plays the predominant role in stabilizing the α-helical conformation, even in the vesicle environment. Furthermore, it appears that when some measure of apo-helicity exists in the absence of PL vesicles, as established for con-T and con-R17 (*14*, *48*), this will not predispose the peptide to further increases in helicity when vesicles are introduced. However, for con-G, the presence of vesicles can enable conversion from the random coil to the helical form, possibly through neutralization of the Gla carboxylates by the quarternary ammonium headgroup of PC.

The structural tendencies of the metal-free forms of con-G, as well as con-T and con-R, were further examined by CD in aligned PL multilayers. The reduction in ellipticity signal intensity at 207 nm manifested by con-T in all multilayer formats (Figure 5B−E) is indicative of a perpendicular orientation to the membrane plane (*49*). In turn, this suggests, but does not necessarily verify, some degree of con-T insertion into the PL layers. In BLPC, con-G and con-R also present spectra consistent with the alignment of their axes normal to the membrane surface. However, in DOPC and DOPC/DOPS, these latter peptides adopt a parallel orientation, with con-R displaying a marked preference for this mode of membrane interaction. A salient difference between BLPC and synthetic DOPC involves the high saturated fatty acid content of the former. Since changes in the orientation preference of helical peptides with the phase state of the lipid have been previously observed (*20*), the more rigid morphology of BLPC multilayers may be promoting the stability of the perpendicular component. These data are not readily reconciled with the results of the fluorescence studies in which the lack of a blue-shift in emmision maximum and only moderate shielding from acrylamide fail to support a model of tyrosine or tryptophan penetration into the lipid bilayer. The oriented CD results imply that the mode of conantokin interaction with the membrane may be dependent upon local features of the asymmetric neuronal membrane environment, including the degree of acyl-chain saturation and membrane fluidity. Furthermore, in recognizing that helix orientation is a dynamic equilibrium, parallel membrane partitioning of the conantokins clearly represents the major equilibrium distribution in solution. However, a small degree of insertion may be occurring, and while undetectable through the solution quenching studies, be thermodynamically favored in certain lipid multilayer formats.

Minor chemical shift deviations (≥±0.12 ppm) are observed for the NH and αCH protons of con-G/Ala, con-G, and con-T in the presence of deuterated vesicles. For the NH resonances, the vesicle-associated shifts are upfield, while all αCH protons manifest downfield shifts. These results argue against peptide insertion into the vesicles and also indicate that no discontinuties in the end-to-end helical character of the peptides occurs when partitioning to vesicles. Intermolecular peptide−lipid NOEs, amide proton exhange rates, and ^{13}C relaxation rates of conantokins in the presence of vesicles clearly reinforce the general conclusion from the fluorescence studies, that the conantokins are localized at the vesicle−buffer interface and do not insert into the vesicle core. This is not unexpected since the high Gla content of the conantokins renders them highly hydrophilic, making insertion into the hydrophobic bilayer energetically unfavorable. However, Gla-domain insertion into the lipid bilayer has been demonstrated for several vitamin K-dependent proteins (*50*−*52*), suggesting that analogous behavior may be occurring in the conantokins. Also, we have recently acquired data that suggest that con-G dimerizes in the presence of physiologically relevant Ca^{2+} concentrations via intermolecular Gla coordination at the dimer interface (Q. Dai, F. J. Castellino, and M. Prorok, manuscript in preparation). This mode of complexation would distribute Leu^5 and Ile^{12} on the outer face of the dimer, allowing for an improved hydrophobic match of these exposed residues with the hydrophobic region of the bilayer. Yet, a lack of a Ca^{2+} effect on the fluorescence and NMR signatures of the conantokins excludes this scenario of dimerization-promoted membrane interaction. Because the Gla residues reside on one face of the helix (*16*), some amphipathic character can be ascribed to the peptides. In this case, another membrane involvement model includes parallel partitioning along the bilayer surface with the charged helix face interacting with the polar lipid headgroups and the more hydrophobic side inserted into the hydrocarbon core (*53*). However, this configuration is not borne out by the NOE determinations. For con-G, con-G/Ala, and con-T, the side chains implicated in contact with

the bilayer surface are equally distributed around the helix perimeter. With respect to relaxation times for select ^{13}C-labeled residues of con-G/Ala, the small decrease in T_2 for the carbonyl carbons of Gly^6 and Ala^{10} in the presence of vesicles suggests some restriction in backbone mobility. In the heptad repeat helix model, these residues occupy neighboring positions f and c, respectively. However, the T_2 values for the side-chain carboxylate carbons of Gla^3 (position c) actually manifest a slight increase upon the addition of vesicles, indicating that no embedding preference exists for that face of the helix. Furthermore, the marginal changes in T_1 and T_2 values not only indicate high mobility of the PL-bound peptide but suggest a rapid exchange of the peptide between the bound and the free state on the NMR time scale. Slower exchange (tighter binding) would be manifested in much longer relaxation times owing to the slow reorientation rates of the vesicles as compared with the peptides.

In conclusion, the conantokins appear to bind the periphery of the membrane bilayer of vesicles in solution and are not embedded beyond the PL headgroups. This mode of membrane binding is reminiscent of class-A amphipathic helices, which partition to the bilayer surface and insinuate no deeper than the ester linkages of the PLs (*21*). Unlike the Gla-containing proteins of the blood coagulation system, the conantokins do not require Ca^{2+} for membrane binding, nor do they exhibit any preference for involvement with acidic PL membranes. In aligned multilayers, con-R17 displays a distinct tendency toward parallel membrane alignment, while con-T adhesion to the membrane has a sizable perpendicular component. The conformation of con-G is intermediate between that of con-R17 and con-T (*14*, *48*). The orientational differences among the conantokins in aligned systems may correlate with the superior NMDAR inhibitory activity of con-R17, which is approximately 5-fold greater than the activity associated with con-G and con-T. The parallel partitioning of con-R17 may allow for faster lateral diffusion along the lipid bilayer, permitting facile access to the NMDAR target.

REFERENCES

1. McIntosh, J. M., Olivera, B. M., Cruz, L. J., and Gray, W. R. (1984) *J. Biol. Chem. 259*, 14343−14346.
2. Haack, J. A., River, J., Parks, T. N., Mena, E. E., Cruz, L. J., and Olivera, B. M. (1990) *J. Biol. Chem. 265*, 6025−6029.
3. White, H. S., McCabe, R. T., Armstrong, H., Donevan, S. D., Cruz, L. J., Abogadie, F. C., Torres, J., Rivier, J. E., Paarmann, I., Hollmann, M., and Olivera, B. M. (2000) *J. Pharmacol. Exp. Ther. 292*, 425−432.
4. Jimenez, E. C., Donevan, S., Walker, C., Zhou, L.-M, Nielsen, J., Cruz, L. H., Armstrong, H., White, H. S., and Olivera, B. M. (2002) *Epilepsy Res. 52*, 73−80.
5. Adams, A. C., Layer, R. T., McCabe, R. T., and Keefe, K. A. (2000) *Eur. J. Pharmacol. 404*, 303−313.
6. Williams, A. J., Dave, J. R., Phillips, J. B., Lin, Y., McCabe, R. T., and Tortella, F. C. (2000) *J. Pharmacol. Exp. Ther. 294*, 378−386.
7. Klein, R. C., Prorok, M., and Castellino, F. J. (2003) *J. Pept. Res. 61*, 307−317.
8. Nelsestuen, G. L., and Lim, T. K. (1977) *Biochemistry 16*, 4164−4171.
9. Kisiel, W., Canfield, W. M., Ericsson, L. H., and Davie, E. W. (1977) *Biochemistry 16*, 5824−5831.
10. Pollock, J. S., Shepard, A. J., Weber, D. J., Olson, D. L., Klapper, D. G., Pedersen, L. G., and Hiskey, R. G. (1988) *J. Biol. Chem. 263*, 14216−14223.
11. Zhang, L., and Castellino, F. J. (1993) *J. Biol. Chem. 268*, 12040−12045.
12. Hall, M. O., Obin, M. S., Prieto, A. L., Burgess, B. L., and Abrams, T. A. (2002) *Exp. Eye Res. 75*, 391−400.
13. Schwyzer, R. (1995) *Biopolymers 37*, 5−16.
14. Prorok, M., Warder, S. E., Blandl, T., and Castellino, F. J. (1996) *Biochemistry 35*, 16528−16534.
15. Colpitts, T. L. and Castellino, F. J. (1993) *Int. J. Pept. Protein Res. 41*, 567−575.
16. Warder, S. E., Blandl, T., Klein, R. C., Castellino, F. J., and Prorok, M. (2001) *J. Neurochem. 77*, 812−822.
17. Klein, R. C., Warder, S. E., Galdzicki, Z., Castellino, F. J., and Prorok, M. (2001) *Neuropharmacology 41*, 801−810.
18. Beals, J. M., and Castellino, F. J. (1986) *Biochem J. 236*, 861−869.
19. Chen, P. S., Jr., Toribara, T. Y., and Warner, H. (1956) *Anal. Chem. 28*, 1756−1758.
20. Clayton, A. H., and Sawyer, W. H. (2000) *Biochim. Biophys. Acta 1467*, 124−130.
21. Clayton, A. H., and Sawyer, W. H. (1999) *Eur. Biophys. J. 28*, 133−141.
22. Wu, Y., Huang, H. W., and Olah, G. A. (1990) *Biophys. J. 57*, 797−806.
23. Huang, H. W., and Olah, G. A. (1987) *Biophys. J. 51*, 989−992.
24. Chen, Y.-H, Yang, J. T., and Martinez, H. M. (1972) *Biochemistry 11*, 4120−4131.
25. Lehrer, S. S., and Leavis, C. P. (1978) *Methods Enzymol. 49*, 222−236.
26. Griesinger, C., Otting, G., Wuthrich, K., and Ernst, R. R. (1988) *J. Am. Chem. Soc. 110*, 7870−7872.
27. Bodenhausen, G., Kogler, H., and Ernst, R. R. (1988) *J. Magn. Reson. 58*, 370−388.
28. States, D. I., Haberkorn, R. A., and Ruber, D. J. (1982) *J. Magn. Reson. 48*, 286−293.
29. Vold, R. L., Waugh, J. S., Klein, M. P., and Phelps, D. E. (1968) *J. Chem. Phys. 48*, 3831−3832.
30. Farrar, T. C., and Becker, E. D. (1978) *Pulsed and Fourier Transform NMR, Introductory to Theory and Methods*, Ch. 2, Academic Press, New York.
31. Weiss, G. H., and Ferretti, J. A. (1988) *Prog. Nucl. Magn. Reson. Spec. 4*, 317−335.
32. Eftink, M. R. (1991) in *Biophysical and Biochemical Aspects of Fluorescence Spectroscopy* (Dewey, T. G., Ed.) pp 1−41, Plenum Press, New York.
33. Follenius, A., and Gerard, D. (1983) *Photochem. Photobiol. 38*, 373−376.
34. Ross, J. B. A., Laws, W. R., Rousslang, K. W., and Wyssbrod, H. R. (1992) *Topics in Fluorescence Spectroscopy* (Lakowicz, J. R., Ed.) Vol. 3, pp 1−63, Plenum Press, New York.
35. Skjærbæk, N., Nielsen, K. J., Lewis, R. J., Alewood, P., and Craik, D. J. (1997) *J. Biol. Chem. 272*, 2291−2299.
36. Klassen, R. B., and Opella, S. J. (1997) *Methods. Mol. Biol. 60*, 271−297.
37. Damberg, P., Jarvet, J., and Graslund, A. (2001) *Methods Enzymol. 339*, 271−285.
38. Glover, K. J., Whiles, J. A., Vold, R. R., and Melacini, G. (2002) *J. Biomol. NMR 22*, 57−64.
39. Williams, K. A., Farrow, N. A., Deber, C. M., and Kay, L. E. (1996) *Biochemistry 35*, 5145−5157.
40. Losonczi, J. A., Olejniczak, E. T., Betz, S. F., Harlan, J. E., Mack, J., and Fesik, S. W. (2000) *Biochemistry 39*, 11024−11033.
41. Kuroda, Y., and Fujiwara, Y. (1987) *Biochim. Biophys. Acta 903*, 395−410.
42. Chen, Z., Blandl, T., Prorok, M., Warder, S. E., Li, L., Zhu, Y., Pedersen, L. G., Ni, F., and Castellino, F. J. (1998) *J. Biol. Chem. 273*, 16248−16258.
43. Warder, S. E., Chen, Z., Zhu, Y., Prorok, M., Castellino, F. J., and Ni, F. (1997) *FEBS Lett. 41*, 19−26.
44. Nelsestuen, G. L., Kisiel, W., and Di Scipio, R. G. (1978) *Biochemistry 17*, 2134−2138.
45. Esmon, C. T., Stenflo, J., Suttie, J. W., and Jackson, C. M. (1976) *J. Biol. Chem. 251*, 3052−3056.
46. Atkins, J. S., and Ganz, P. R. (1992) *Mol. Cell Biochem. 112*, 61−71.
47. Burstein, E. A., Vedenkina, N. S., and Ivkova, M. N. (1973) *Photochem. Photobiol. 18*, 263−279.
48. Blandl, T., Zajicek, J., Prorok, M., and Castellino, F. J. (2001) *J. Biol. Chem. 276*, 7391−7396.

49. de Jongh, H. H. J., Goormaghtigh, E., and Killian, J. A. (1994) *Biochemistry 33*, 14521−14528.
50. Zhang, L., and Castellino, F. J. (1994) *J. Biol. Chem. 269*, 3590−3595.
51. Falls, L. A., Furie, B. C., Jacobs, M., Furie, B., and Rigby, A. C. (2001) *J. Biol. Chem. 276*, 23895−23902.
52. Harvey, S. B., Stone, M. D., Martinez, M. B., and Nelsestuen, G. L. (2003) *J. Biol. Chem. 278*, 8363−8369.
53. Heller, W. T., He, K., Ludtke, S. J., Harroun, T. A., and Huang, H. W. (1997) *Biophys. J.* 73, 239−244.

BI034918P